Degradation of a xanthene dye by Fe(II)-mediated activation of Oxone process

Y.R. Wang, W. Chu*

Department of Civil and Structural Engineering, Research Centre for Urban Environmental Technology and Management, The Hong Kong Polytechnic University, Hung Hom, Kowloon, Hong Kong

ARTICLE INFO

ABSTRACT

A powerful oxidation process using sulfate radicals activated by transition metal mediated Oxone process has been evaluated in depth by monitoring the degradation of a xanthene dye Rhodamine B (RhB) in aqueous solution. Ferrous ion was chosen as the transition metal due to its potential catalytic effect and wide availability in dyeing industrial effluent. The effects of parameters including reactant dosing sequence, Fe(II)/Oxone molar ratio and concentration, solution pH, and inorganic salts on the process performance have been investigated. Total RhB removal was obtained within 90 min under an optimal Fe(II)/Oxone molar ratio of 1:1. The RhB degradation was found to be a two-stage kinetics, consisting of a rapid initial decay and followed by a retarded stage. Additionally, experimental results indicated that the presence of certain anions had either a positive or negative effect on the process. The inhibitory effect in the presence of SO_4^{2-} was elucidated by a proposed formula using Nernst equation. Furthermore, dye mineralization in terms of TOC removal indicates that stepwise addition of Fe(II) and Oxone can significantly improve the process performance by about 20%, and the retention time required can be greatly reduced comparing with the conventional one-off dosing method.
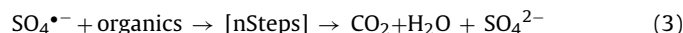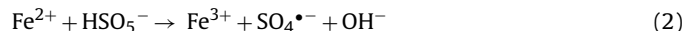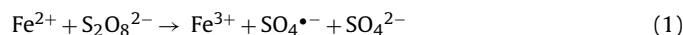
© 2010 Elsevier B.V. All rights reserved.

1. Introduction

It is estimated that around 10^6 tons of commercially different dyes are produced annually world-wide and about 5–10% of the dyestuffs are lost in the industrial effluents [1] with a concentration varying from the range of 10–10,000 mg L^{-1} [2]. The complex structures and stable properties make most of the dyes resistant to biological degradation and photodegradation [3,4] and some of them are even toxic, carcinogenic and mutagenic [5]. In addition, color caused by dye contaminants interferes with penetration of sunlight into waters, retards photosynthesis, inhibits the growth of aquatic biota and interferes with gas solubility in water bodies [6]. As a result, various treatment techniques have been investigated and developed to decolorize and/or degrade dye contaminants [7], including electro-oxidation [8], advanced oxidation processes (AOPs) [9], adsorption [10,11], biological degradation and filtration processes [12], and so on.

Advanced oxidation processes (AOPs) are considered to be one of the most effective methods due to the generation of highly reactive radicals. AOPs involve the utilization of sole or combined high oxidation potential oxidants such as ozone, hydrogen peroxide, persulfate, ferrate(VI), sometimes coupled with UV radiation and/or specific catalysts. Fenton's process by coupling H_2O_2 with

a transition metal (Fe^{2+}) is a rapid and inexpensive process [13]. However, the requirement of low pH environment is the major limitation [14]. On the basis of the Fenton's process, sulfate radicals ($SO_4^{\bullet-}$) generated by the combination of oxidants (persulfate or peroxymonosulfate) with transition metals (Fe^{2+}, Ag^+, Co^{2+}) demonstrate higher standard reduction potential at neutral pH [14,15]. Anipsitakis and Dionysiou have reported that sulfate radicals are more efficient than hydroxyl radicals at least for the transformation of 2,4-dichlorophenol, atrazine, and naphthalene under certain conditions [16]. The $SO_4^{\bullet-}$ generation mechanism and its interaction with organic compounds were reported by previous studies [15–18]:

$$Fe^{2+} + S_2O_8^{2-} \rightarrow Fe^{3+} + SO_4^{\bullet-} + SO_4^{2-} \tag{1}$$

$$Fe^{2+} + HSO_5^- \rightarrow Fe^{3+} + SO_4^{\bullet-} + OH^- \tag{2}$$

$$SO_4^{\bullet-} + organics \rightarrow [nSteps] \rightarrow CO_2 + H_2O + SO_4^{2-} \tag{3}$$

where the end product SO_4^{2-} is practically inert and is considered environmental benign. Therefore, persulfate and peroxymonosulfate, as an oxidant alternative for the degradation of organic contaminants, have received considerable attention in recent years.

Oxone ($2KHSO_5 \cdot KHSO_4 \cdot K_2SO_4$), a triple salt compound, is the source providing peroxymonosulfate (HSO_5^-) which is reported to be a more efficient oxidant than hydrogen peroxide or persulfate [19]. Therefore, Oxone was chosen as the oxidant source in this study. To activation the relatively stable Oxone in generation $SO_4^{\bullet-}$, Anipsitakis et al. (2004) demonstrated that Co^{2+} is an efficient tran-
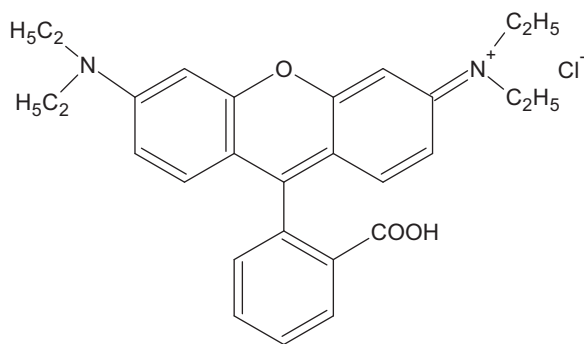
Fig. 1. Chemical structure of Rhodamine B.

sition metal to trigger the process at neutral pH. Nevertheless, cobalt (II) has been shown to be toxic and slightly carcinogenic upon inhalation in mice and might result in environmental concern when discharged along with the effluent. Thus, Fe^{2+} which shows considerable activation of Oxone and commonly exists in printing and dyeing industrial effluent was selected as the transition metal in this work.

Rhodamine B (RhB), a water-soluble xanthene dye and famous for its good stability as dye laser materials [20], is widely used in dyestuff industries and modern photochemistry, and most important it is a suspected carcinogen [21,22]. Therefore, the degradation of RhB by sulfate radicals generated based on the Fe(II)-mediated Oxone process was explored in this study.

In this work, the performance of Fe(II)/Oxone process was evaluated. Effects of some critical parameters, including transition metal and oxidant concentration, solution pH, and different electrolytes on the dye degradation efficiency were investigated. Moreover, the mineralization behavior of RhB in the Fe(II)/Oxone process was also evaluated by monitoring the TOC decrease under the selected experimental conditions.

2. Materials and methods

2.1. Chemicals

The commercially available dye Rhodamine B obtained from Sigma Aldrich Inc (C.I. name: Basic violet10; Formula: $C_{28}H_{31}N_2O_3Cl$; Formula weight: 479.01) at 90% is used as the probe without further purification, its chemical structure was illustrated in Fig. 1. All the other chemicals used in this study, including Oxone ($2KHSO_5 \cdot KHSO_4 \cdot K_2SO_4$, 1 M Oxone provides 2 M HSO_5^-; Formula weight: 614.7; DuPont product), ferrous sulfate ($FeSO_4 \cdot 7H_2O$, 99.0%), sodium sulfate (Na_2SO_4, 99.0%), sodium nitrate ($NaNO_3$, 99.5%), and sodium chloride ($NaCl$, 99.5%), are analytical grade and purchased from Sigma–Aldrich Inc. (USA). All the solutions were prepared in deionized and distilled water with a resistivity of 18.2 MΩ from a Bamstead NANOpure water treatment system (Thermo Fisher Scientific Inc., USA).

2.2. Experimental procedures

The degradation experiments were performed at air-conditioned room temperature (at $23 \pm 2\,^\circ C$) in 50 mL batch reactors. RhB stock solution (1.0 mM) was prepared in deionized distilled water and specific aliquots of the solution were added into the reactors to achieve a predetermined initial concentration. The Fe(II) and Oxone solutions were freshly prepared before each experiment to minimize variations in concentration caused by precipitation, oxidation of ferrous solution and self-decomposition of oxidant. In addition, the Fe(II) solution was prepared in degassed

H_2SO_4 solution at pH 3 to prevent Fe(II) from precipitation and/or oxidation. The reactions were initiated by pipetting appropriate amounts of Fe(II) and Oxone into the reactor to achieve the predefined molar ratios of RhB:Fe(II):Oxone. The initial volume of the reaction solution was fixed at 50 mL. The pH values were adjusted with 0.10 M nitric acid and/or 0.10 M sodium hydroxide whenever required. At predetermined time intervals, the sample aliquots were withdrawn from the reactor and mixed immediately with appropriate amounts of methanol (0.5 mL) to quench the reaction. The solution was then analyzed by High Performance Liquid Chromatography (HPLC) to quantify the remaining dye. For TOC measurement, sodium sulfite, an inorganic salt, was chosen as the quencher to minimize any interference of quenching agent in TOC analysis. All the experiments were carried out in duplicate and the data presented in this study have errors less than 3%.

2.3. Analytical procedures

The HPLC is consisted of a Waters 515 HPLC pump, a Waters 2489 UV/Visible Detector and a Water 717 plus Autosampler. The chromatographic separations were performed on a Pinnacle DB C18 reversed phase column (250 mm × 4.6 mm with i.d. of 5 μm) from RESTEK. The mobile phase was composed of 60% acetonitrile and 40% water (V/V). The flow rate was 1 mL min^{-1} and injection volumes were 10 μL. Retention time for RhB was 6.0 min at the above conditions. The UV/Visible Detector was set at 553 nm, which was the maximum absorbance wavelength of RhB solution and determined by scanning the spectra of the tested samples from 200 nm to 900 nm using a spectrophotometer Spectronic (R) GenesysTM with a 1 cm path length spectrometric quartz cell.

For comparison, the decolorization of RhB was also determined by monitoring decrease in absorbance at the maximum wavelength (553 nm) using UV–vis spectrophotometer.

TOC was measured by a Shimadzu TOC-5000A analyzer equipped with an ASI-5000A autosampler to identify the mineralization of the organic contaminants. The solution pH level was determined by a CD510 digital pH meter.

3. Results and discussion

3.1. Dosing sequence of reactants

Initially, control experiments were conducted to determine the RhB removal solely by ferrous sulfate or Oxone. As the ratio of Fe(II)/RhB is 10, the [RhB] remained the same throughout the whole process (90 min), under the same condition, 5% of [RhB] decay was observed at a ratio of Oxone/RhB of 5. Accordingly, it can be concluded that the dye degradation by sole ferrous or Oxone is negligible as shown in Fig. 2.

There are two critical reagents involved in the Fe(II)/Oxone system, experiments were therefore performed to verify the effect of reactant dosing sequence on the dye degradation. Two tests were conducted, one was by adding ferrous sulfate (as a source of ferrous ions) into RhB solution and followed by adding Oxone to initiate the reaction, and the other was by adding Oxone first then ferrous sulfate. It is interesting to note that Fe(II)-Oxone addition demonstrates a better and faster dye degradation performance, even when the two dosages were separated by 30 s apart, as shown in Fig. 2. The overall RhB removal was 60% and 50% for Fe(II)-Oxone and Oxone-Fe(II) addition, respectively; indicating that the Fe(II)-Oxone addition showed a higher dye degradation performance. This might be attributed to two reasons: although the non catalyst-mediated decomposition of Oxone is slow, there was still a portion of Oxone directly react with the dye when the oxidant (Oxone) was added first (as justified in Fig. 2, the 5% removal). In addition, the
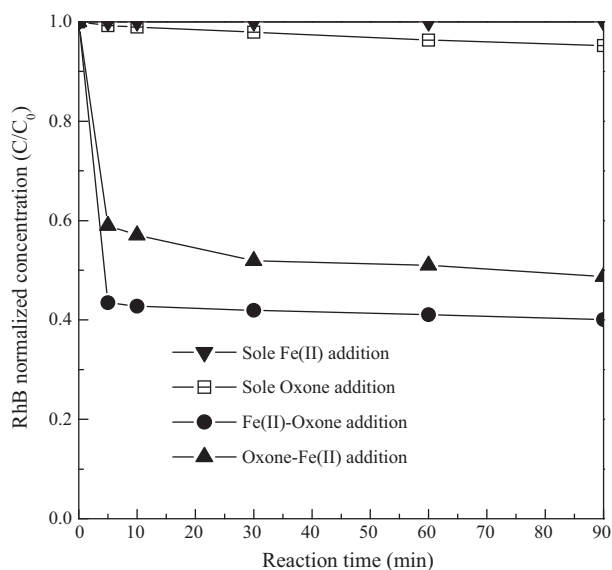
Fig. 2. Effect of reactants adding order on RhB degradation. Experimental conditions were 0.02 mM $[RhB]_0$, 0.20 mM $[Fe(II)]_0$, and 0.10 mM $[Oxone]_0$ (which provides 0.2 mM peroxymonosulfate ions) without pH adjustment.

RhB used in this experiment was a commercial dye coming with about 10% of impurity, the added Oxone (in the form of HSO_5^-) may also react with these impurities. The existence of sulfate radicals as major oxidizing species in Fe(II)-mediated activation of Oxone system has been verified previously [18]. It is likely that these two reasons might result in a lower generation of sulfate radicals in the later Fe(II)/Oxone process upon the addition of Fe(II). In the case of Fe(II)-Oxone addition, once the oxidant was dosed into the reactor, large amounts of $SO_4^{\bullet-}$ were instantaneously generated in the presence of the previous added catalyst (Fe(II)). Because sulfate radicals are more selective for oxidation via electron transfer than that of hydroxyl radicals [23], it can be speculated that the higher degradation efficiency was likely due to the preferred selective oxidation reaction between sulfate radical and RhB. Fe(II)-Oxone addition sequence was therefore adopted in the remaining study.

3.2. Effect of Fe(II): Oxone ratio on RhB degradation

In the Fe(II)/Oxone system, Fe(II) was used as the transition metal for the activation of Oxone to generate the radicals. Thus, the generation of $SO_4^{\bullet-}$ can be affected by the molar ratio and/or the concentration of Fe(II) and Oxone. Optimum Fe(II)/Oxone molar ratio was identified by varying Fe(II)/Oxone ratios ranging from 1:10 to 10:1 with constant [Oxone] at 0.10 mM and 0.20 mM, respectively.

Dye degradation at different Fe(II)/Oxone molar ratios was depicted in Fig. 3, where two different types of reaction were identified. When the Fe(II)/Oxone ≤ 1, the RhB showed a rapid degradation in the first 5 min and then followed by a much slower decay, i.e. a two-stage reaction consisting of a rapid degradation stage followed by a retarded slow reaction. Additionally, the rate constants of both stages increased as Fe(II)/Oxone ratio increased until 1:1 was reached. The removal efficiency increased from 23.7% to 63.3% for Fig. 3(a) and from 31.6% to 100% for Fig. 3(b) with [Oxone] at 0.10 and 0.20 mM, respectively.

However, as the ratio Fe(II)/Oxone > 1, the dye concentration in the solution dropped sharply within the first few minutes and then the curves leveled off, suggesting the reaction was completed right after the reaction was started. This observation is very useful for real application, especially if the space available for a large reactor is limited.
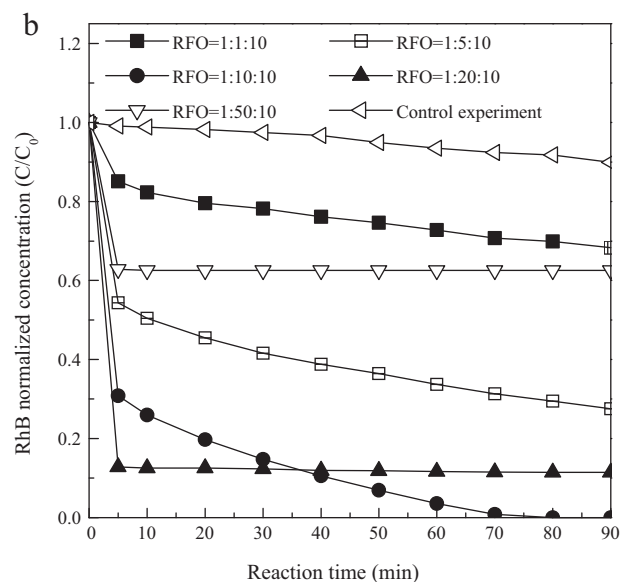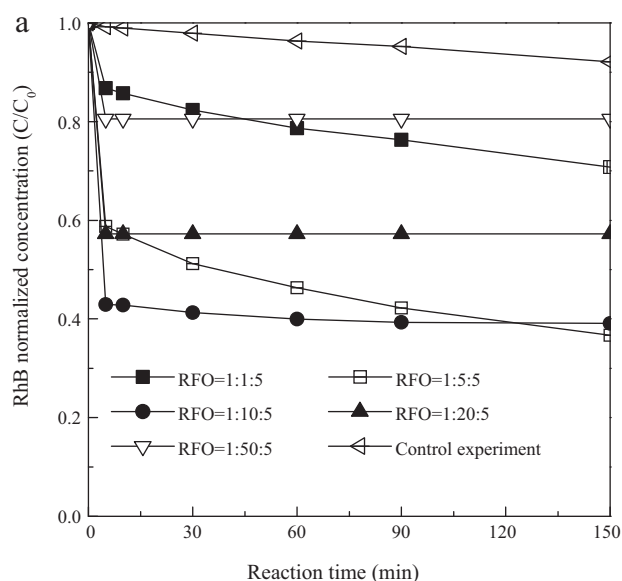
Fig. 3. Effect of different ratios of RhB:Fe(II):Oxone (RFO) on dye degradation. Conditions were (a) 0.02 mM $[RhB]_0$ and 0.10 mM $[Oxone]_0$; (b) 0.02 mM $[RhB]_0$ and 0.20 mM $[Oxone]_0$.

To optimize the process, the decay curves were further analyzed as shown in Fig. 4, where the dye decay at a specific reaction time is apparently a function of the Fe(II)/Oxone ratio. In general, the closer the ratio to 1, the better the degradation efficiency of the system. Moreover, the higher the Oxone concentration, the faster the decay rate as well as the higher the performance for the fixed catalyst and oxidant molar ratio. In this study, 100% dye degradation was observed within 90 min when the ratio of Fe(II)/Oxone was 1 and the Oxone was fixed at 0.20 mM.

In the Fe(II)-mediated Oxone process, sulfate radical was generated through the decomposition of Oxone catalyzed by the Fe(II) via Eq. (2). Compared with Fenton's reaction which has a reaction rate constant around $k = 53$–$76\,M^{-1}\,s^{-1}$ [24], Eq. (2) has a much higher reaction rate constant of $k = 3.0 \times 10^4\,M^{-1}\,s^{-1}$ [18], indicating a faster generation of sulfate free radicals once Oxone is in contact with Fe(II). Large amounts of $SO_4^{\bullet-}$ were responsible for the rapid dye degradation in the first few minutes. The ferric ions generated in Eq. (2) would serve as an electron acceptor and further decompose extra Oxone to generate peroxysulfate radicals,
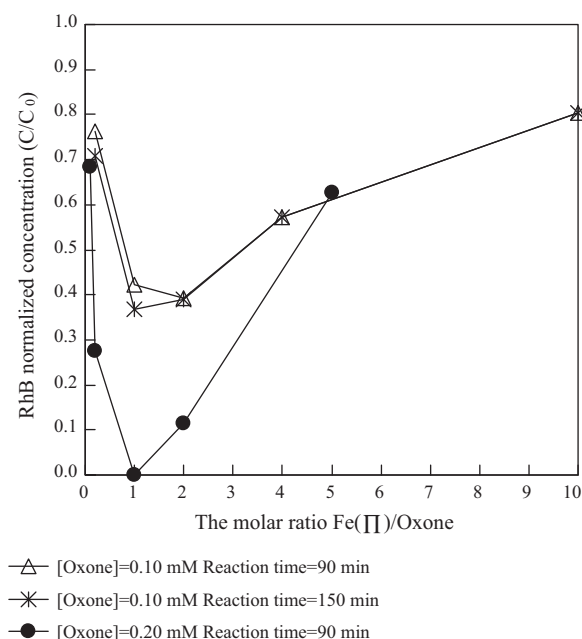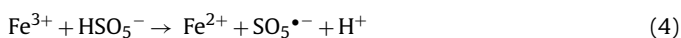
Fig. 4. Degradation performance as a function of Fe(II)/Oxone molar ratio.

which are a weaker oxidant than the sulfate radicals via the Eq. (4) expressed as follow:

$$Fe^{3+} + HSO_5^- \rightarrow Fe^{2+} + SO_5^{\bullet-} + H^+ \qquad (4)$$

Ferrous ions regenerated through Eq. (4) will further react with Oxone. However, compared with the Fe(II)/Oxone system, previous study showed that the coupling of Fe(III) with Oxone showed a much lower rate in degrading organics [16]. This also confirms with the slower second-stage reactions in Fig. 3 as Fe(II)/Oxone ≤1. This observation indicates that Fe(II) ions are consumed much more rapidly than they are re-produced. On the other hand, excessive Fe(II) in Fe(II)/Oxone system can act as a sulfate-radical scavenger through Eq. (5) which has a far higher rate constant of $k = 3.0 \times 10^8 \, M^{-1} \, s^{-1}$ than that of Eq. (2).

$$Fe^{2+} + SO_4^{\bullet-} \rightarrow Fe^{3+} + SO_4^{2-} \qquad (5)$$

Therefore, unlimited increase of Fe(II) in the process is not recommended. In this study, it can be concluded that when the molar ratio Fe(II)/Oxone ≤1, the rapid first-stage is mainly due to the rapid sulfate radical generation that reacts with dye molecule; while the slower second-stage is likely hindered by the combination of lower sulfate radicals in the solution, the weaker peroxysulfate radicals produced by Fe(III)/Oxone and slow reactivation of Fe(II) catalyst. RhB was degraded mainly through the oxidizing radicals generated via Eqs. (2) and (4) under this condition. Whereas, in the presence of an excessive amount of Fe(II), especially when the molar ratio Fe(II)/Oxone is higher than 2 (from Fig. 3), a sudden drop of the [RhB] and a lowered overall RhB decay was observed. The former is due to the rapid sulfate radicals' generation by the excessive ferrous ions, while the latter is due to the futile-consumption of $SO_4^{\bullet-}$ by excess Fe(II) as indicated in Eq. (5).

3.3. Effect of pH level on RhB degradation

The effects of initial solution pH on RhB degradation were explored in an extensive pH range from 2.67 to 10.22 at its optimum Fe(II)/Oxone ratio of 1:1 and the results were illustrated in Figs. 5 and 6, where RhB degrading performance directly depended on the initial solution pH. Optimal dye removal efficiency was observed at an initial pH around 3.5, above or below this pH level,
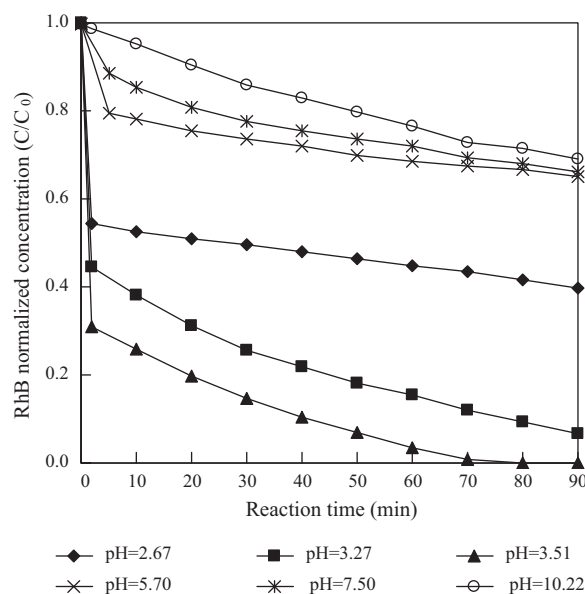

Fig. 5. Effect of initial solution pH after adding Oxone. Experimental conditions were set at 0.02 mM [RhB]$_0$ with RFO molar ratio of 1:10:10.

the process performance reduced. Due to the presence of acidic bisulfate in Oxone, the solution pH would drop sharply after adding Oxone to the process. The pH variation before and after Oxone addition was monitored and depicted in the inset of Fig. 6, where Oxone addition resulted in a solution pH of 3.51 if no pH adjustment.

The decrease of dye removal efficiency at lower pH range is most likely attributed to the formation of $(Fe(II)(H_2O))^{2+}$ at low pH levels [25], which results in a decrease of free [Fe(II)] in the solution. On the other hand, dye removal performance also dropped rapidly when the initial solution pH increased to higher pH level (from pH 3.51 to 10.22). This can be rationalized by two mechanisms. First, the instability of ferrous ions at the pH level higher than 4.0 led to the formation of ferrous/ferric hydroxide complexes (i.e. iron precipitation), which have a lower catalytic activity and thus have a negative impact on the sulfate radical generation. As shown in Fig. 5, the rapid first-stage kinetics no longer exists at extremely
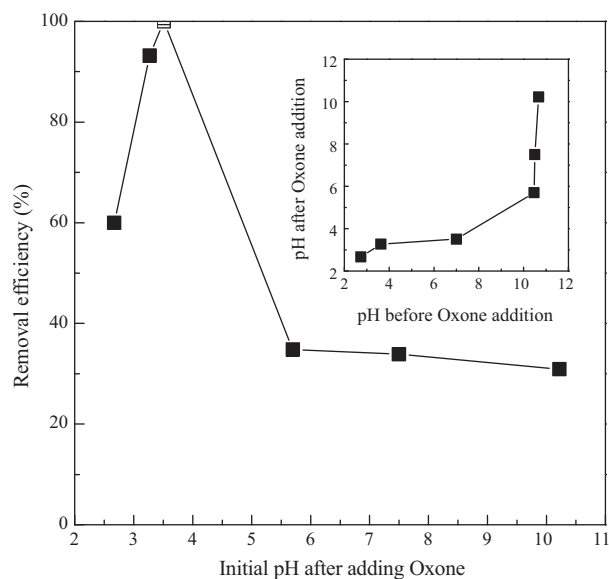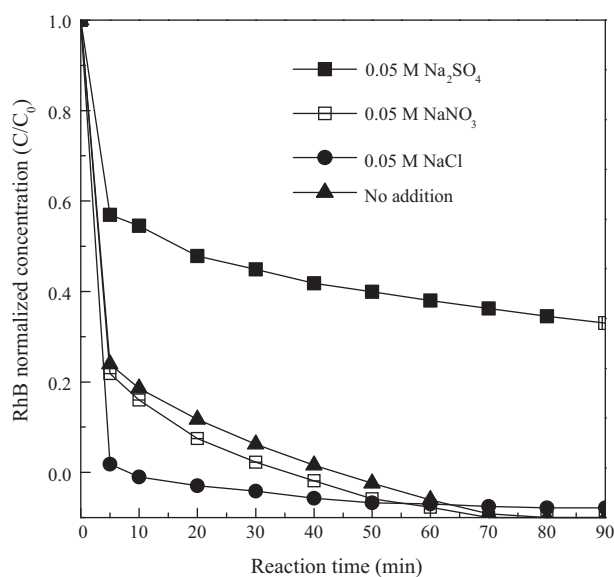

Fig. 6. Degradation performance as a function of initial solution pH after adding Oxone. Experimental conditions were set at 0.02 mM [RhB]$_0$ with RFO molar ratio of 1:10:10.
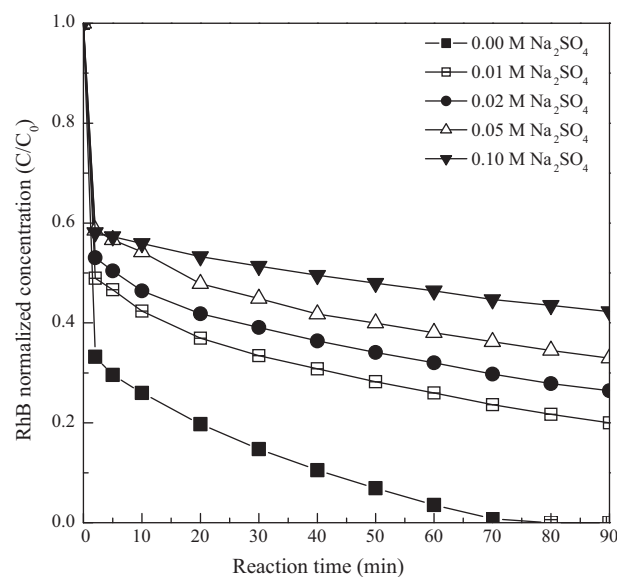
Fig. 7. Effect of inorganic salts: NaCl, NaNO₃, Na₂SO₄. Experimental conditions were set at 0.02 mM [RhB]₀ with RFO molar ratio of 1:10:10 without pH adjustment.

Fig. 8. Effect of ionic strength: Na₂SO₄. Experimental conditions were set at 0.02 mM [RhB]₀ with RFO molar ratio of 1:10:10 without pH adjustment. Na₂SO₄ was added in different amount.

high pH level of 10.22, indicating a deficiency of catalyst. Second, self-dissociation of Oxone at a raised pH level was reported and was observed mainly through non-radical pathways [18,26], which would impair the oxidizing capacity of Oxone towards the probe contaminant. Consequently, an optimal solution pH of 3.5 was recommended for the RhB removal. This is convenient for wastewater treatment because no pH adjustment is required.

3.4. Effect of various inorganic salts

Large amounts of additives and mordants, including inorganic salts, have been utilized in the dyeing process, which resulted in a complex wastewater and imposed a significant influence on its treatment. The performances of degrading RhB by using three different inorganic salts (Na₂SO₄, NaNO₃, and NaCl at 0.05 M) were evaluated by comparing with control (without electrolyte), and the results were shown in Fig. 7. It can be noted that the NaCl, Na₂SO₄, and NaNO₃ show improved, retarded, and null effects on the dye's degradation with about 91%, 43%, and 71% RhB removal in 5 min, respectively.

In-depth analysis of Na₂SO₄ and NaCl on the dye removal were therefore conducted to elucidate the role of SO_4^{2-} and Cl^- in the Fe(II)/Oxone process by varying the [Na₂SO₄] and [NaCl] from 0.0 to 0.1 M. For the SO_4^{2-}, as shown in Fig. 8, both the first- and second-stage RhB decay rates were decreased with the increment of [Na₂SO₄]. One possible explanation is that the decomposition of Oxone is likely inhibited by the high-ionic strength (IS) of the solution. As reported by Kolthoff and Miller, the persulfate decomposition rate in a 0.1 M of $HClO_4$ solution decreased with the increase of IS [27], while Huang et al. found that the higher the IS, the slower MTBE degraded by persulfate [28]. However, it is interesting to note that 0.05 M NaNO₃ (giving an IS of 0.05 M) has a higher IS than that of 0.01 M Na₂SO₄ (with an IS of 0.03 M), but the latter demonstrates much higher rate inhibition than the former. Thus, the use of IS alone to justify the retardation effect is not enough. Assuming the reactions involving the consumption of sulfate free radicals (Eq. (3)) can be simplified into

$$SO_4^{\bullet-} + e^- \rightarrow SO_4^{2-} \tag{6}$$

the corresponding Nernst equation of Eq. (6) then can be formulated as (Logic)

$$E(SO_4^{\bullet-}) = E^{\theta}_{(SO_4^{\bullet-}/SO_4^{2-})} + \frac{RT}{zF} \ln \frac{[SO_4^{\bullet-}]}{[SO_4^{2-}]} \tag{7}$$

where, $E_{(SO_4^{\bullet-}/SO_4^{2-})}$ is the half-reaction reduction potential, $E^{\theta}_{(SO_4^{\bullet-}/SO_4^{2-})}$ represents the standard half-reaction reduction potential, R is the universal gas constant 8.314472 J K⁻¹ mol⁻¹, T is the absolute temperature, F is the Faraday constant 9.6485×10^4 C mol⁻¹, z is the number of electrons transferred in the half-reaction. According to the Eq. (7), it can be seen that the redox potential of $SO_4^{\bullet-}/SO_4^{2-}$ can be affected by the concentration of SO_4^{2-}. Higher the [SO_4^{2-}], lower the $E_{(SO_4^{\bullet-}/SO_4^{2-})}$, which directly lower the performance of dye oxidation. Assuming a complete generation of $SO_4^{\bullet-}$ can be achieved through Eq. (2) in the first-stage, it can be calculated that $E_{(SO_4^{\bullet-}/SO_4^{2-})}$ will be reduced by 0.1363 V when [SO_4^{2-}] increased from 0.010 M to 0.10 M under the tested conditions. This was consistent with the reported redox potential of sulfate radicals, which varies from 2.5 to 3.1 V depending on the reaction conditions [29].

Fig. 9 illustrates the effect of [NaCl] in the Fe(II)/Oxone system. It can be noted that the first-stage degradation rate was accelerated as [Cl^-] increased. It is interesting to note that the chloride ion can still improve the dye degradation even in the absence of Fe(II), as shown in Fig. 10, where more than 93% of dye was degraded within 50 min at a high [Cl^-]. As expected, the degradation rates of RhB by Cl^-/Oxone/Fe(II) were about 200–3.5 times faster than that of Cl^-/Oxone as [Cl^-] increased from 0.001 to 0.1 M.

It was known that chloride ions can be oxidized by sulfate radicals to form chlorine radicals via Eq. (8) [30], which may resulte in a series of secondary oxidants as indicated in Eqs. (9)–(13). In addition, Cl^- can be oxidized thermodynamically by HSO_5^- (1.75–1.8 V) to form chlorine ($Cl_2/2Cl^-$, 1.36 V) and hypochlorous acid ($HOCl/Cl^-$, 1.48 V) as also verified by others [31,32]. These secondary oxidants are likely to contribute and improve the dye's decay by offering parallel decay pathways, which may involve the reactions of chlorine radicals (Eq. (16)) and free available chlorine

Fig. 9. Effect of ionic strength: NaCl. Experimental conditions were set at 0.02 mM [RhB]$_0$ with RFO molar ratio of 1:10:10 without pH adjustment. NaCl was added in different amount.
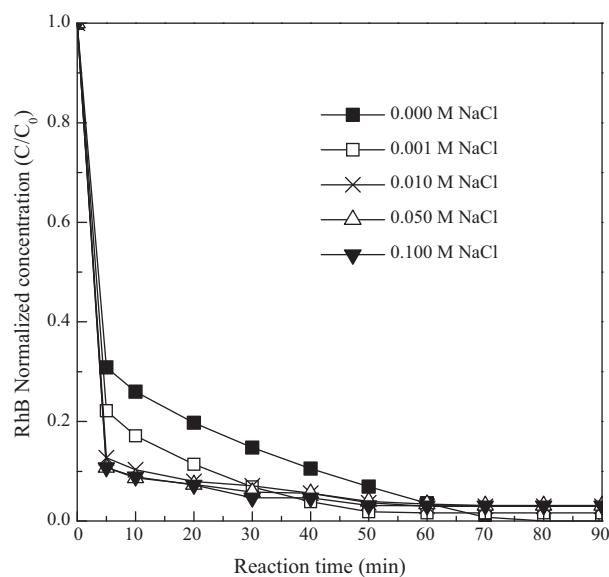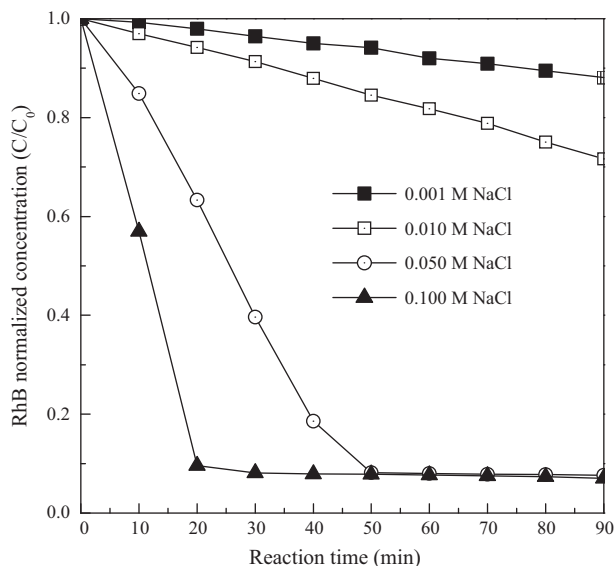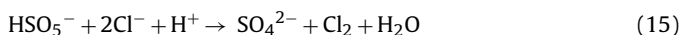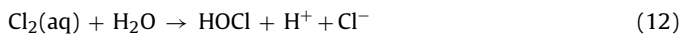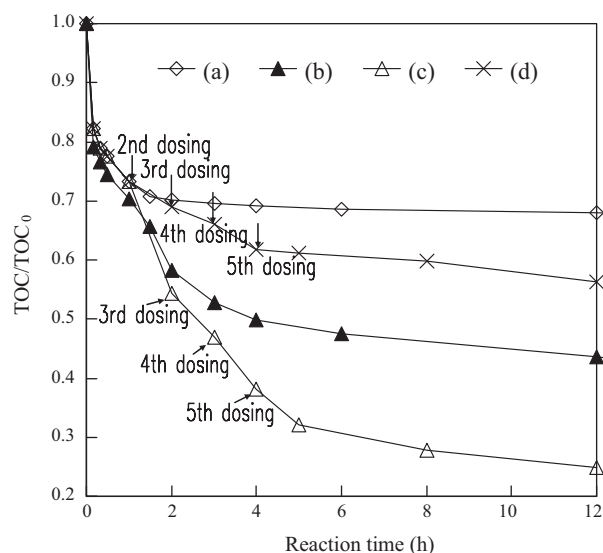

Fig. 11. TOC removal as a function of reaction time. Experimental conditions: [RhB]$_0$ = 0.10 mM; Without pH adjustment. (a) RFO = 1:10:10; (b) RFO = 1:50:50; (c) RFO = 1:50:50, stepwise addition of Fe(II) and Oxone; (d) RFO = 1:10:50, stepwise addition of Oxone.

species (Eq. (17)).

$$SO_4^{\bullet-} + Cl^- \rightarrow SO_4^{2-} + Cl^\bullet \qquad (8)$$

$$Cl^\bullet + Cl^- \rightarrow Cl_2^{\bullet-} \qquad (9)$$

$$Cl_2^{\bullet-} + Cl_2^{\bullet-} \rightarrow Cl_2 + 2Cl^- \qquad (10)$$

$$Cl^\bullet + Cl^\bullet \rightarrow Cl_2 \qquad (11)$$

$$Cl_2(aq) + H_2O \rightarrow HOCl + H^+ + Cl^- \qquad (12)$$

$$HOCl \rightarrow {}^-OCl + H^+ \qquad (13)$$

$$HSO_5^- + Cl^- \rightarrow SO_4^{2-} + HOCl^- \qquad (14)$$

$$HSO_5^- + 2Cl^- + H^+ \rightarrow SO_4^{2-} + Cl_2 + H_2O \qquad (15)$$

$$R^\bullet + Cl_2^{\bullet-} \rightarrow R–Cl + Cl^- \qquad (16)$$

$$R–H + HOCl \rightarrow R–Cl + H_2O \qquad (17)$$

Fig. 10. Effect of Cl$^-$ on the RhB degradation. Experimental conditions were 0.02 mM [RhB]$_0$, 0.20 mM [Oxone]$_0$ without Fe(II) and pH adjustment.

It was reported that para-selective oxychlorination of aromatic compounds is favored by the combination of Oxone with chloride [33]. Thus, the faster degradation of RhB by the Fe(II)/Oxone/Cl$^-$ process may be partly attributed to the favorable chlorination on the aromatic ring of RhB through Eqs. (8)–(17). However, for the Oxone/Cl$^-$ process, the degradation of RhB is mainly through the non-radical reactions, i.e. Eqs. (13)–(17), which results in a slower reaction rate.

The positive effect by increasing [Cl$^-$] in the Fe(II)/Oxone system on RhB degradation may not be suitable for the treatment of other types of wastewater, because some chlorinated by-products formed during the chlorination process may be difficult to be further oxidized or become more toxic. A careful evaluation on each type of wastewater is recommended.

3.5. Mineralization of RhB

Mineralization of RhB in the Fe(II)/Oxone process was assessed by measuring the decrease in TOC with an initial RhB concentration of 0.10 mM or 33.6 mg L^{-1} TOC as calculated stoichiometrically by Eq. (18).

$$C_{28}H_{31}ClN_2O_3 + 73KHSO_5 \rightarrow 28CO_2 + 14H_2O + Cl^- + 2NO_3^-$$
$$+ 3H^+ + 73KHSO_4 \qquad (18)$$
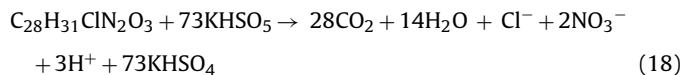
The removal of RhB under the molar ratio of RhB:Fe(II):Oxone (RFO) at 1:10:10 was found to be efficient as discussed previously. Under these circumstances, however, it was found inefficient for TOC removal, where only 30% TOC was removed, as shown in Fig. 11. This result is reasonable considering the ratio of RFO at 1:10:10 is far less than the required stoichiometric dosage for complete mineralization as indicated in Eq. (18). Thus, the tailing of TOC curve is likely attributed to the depletion of Oxone. This can be justified by increasing the RFO ratio to 1:50:50, and that the abatement of TOC was most efficient in the early stage of the reaction and significantly slowed down afterward. This is likely due to the inefficient side reactions of ferrous and Oxone as discussed before. To minimize the involvement of side reactions, it's possible to modify the conventional process into a stepwise dosing approach. For the same RFO ratio at 1:50:50, the oxidant and catalyst were evenly distributed into 5 dosages at 1 h apart. As shown in Fig. 11 (curve

c), the total TOC removal further increased to 75%, which is 20% higher than that of one-off dosing process. In addition, it should be noted that the stepwise addition is 4 times faster to achieve the same level of TOC removal (i.e. 55%) than that of one-off dosing. This is critical for a treatment plant design, since a much smaller reactor can be used for a specific performance.

The role of Fe(II) in the stepwise approach was investigated as well. It was carried out by initiating the reaction at a RFO ratio 1:10:10, then the additional Oxone was dosed into the reactor in stepwise until the final RFO reached 1:10:50, as shown as the curve d in Fig. 11. Compared with the curve c (RFO = 1:50:50), TOC removal of the curve d reduced to 44%, which was much smaller than that of the curve c (75%). This suggests that the slow regeneration of ferrous ions can not support the fast oxidation reactions in time. It is necessary to maintain Fe(II) level during the stepwise process to ensure effective and rapid mineralization.

4. Conclusions

The degradation of RhB was investigated using $SO_4^{\bullet-}$ generated by the coupling of Oxone and ferrous ions as oxidant and transition metal, respectively. Experimental results showed that the performance of dye degradation was dramatically influenced by operating parameters, such as the molar ratio and the concentration of Fe(II) and Oxone, initial solution pH, and inorganic salts. Optimum molar ratio of Fe(II)/Oxone was identified to be 1:1. Furthermore, the results indicated the higher the Oxone concentration, the faster the decay rate as well as the higher the performance. Optimum dye removal efficiency was observed at an initial solution pH of 3.51 within the investigated pH range of 2.67–10.22. The overall dye degradation can be described as a two-stage reaction consisting of a rapid degradation stage followed by a retarded reaction stage under the optimum conditions. In addition, the presence of certain anions had a significant effect on the Fe(II)/Oxone process. It was found that SO_4^{2-} demonstrated adverse effect in the process, whereas the existence of Cl^- facilitated the transformation of RhB. The mineralization of RhB is feasible and the performance can be greatly improved by using stepwise Fe(II) and Oxone dosing approach.

References

[1] M.A. Sanroman, M. Pazos, M.T. Ricart, C. Cameselle, Decolourization of textile indigo dye by DC electric current, Eng. Geol. 77 (2005) 253–261.
[2] S. Figueroa, L. Vazquez, A. Alvarez-Gallegos, Decolorizing textile wastewater with Fenton's reagent electrogenerated with a solar photovoltaic cell, Water Res. 43 (2009) 283–294.
[3] A.K. Mittal, C. Venkobachar, Uptake of cationic dyes by sulfonated coal: sorption mechanism, Ind. Eng. Chem. Res. 35 (1996) 1472–1474.
[4] Z.H. Ai, L.R. Lu, J.P. Li, L.Z. Zhang, J.R. Qiu, M.H. Wu, Fe@Fe2O3 core-shell nanowires as iron reagent. 1. Efficient degradation of Rhodamine B by a novel sono-Fenton process, J. Phys. Chem. C 111 (2007) 4087–4093.
[5] G.C. Panda, S.K. Das, A.K. Guha, Jute stick powder as a potential biomass for the removal of congo red and rhodamine B from their aqueous solution, J. Hazard. Mater. 164 (2009) 374–379.
[6] S.R. Couto, Dye removal by immobilized fungi, Biotechnol. Adv. 27 (2009) 227–235.
[7] E. Forgacs, T. Cserhati, G. Oros, Removal of synthetic dyes from wastewaters: a review, Environ. Int. 30 (2004) 953–971.
[8] D. Dogan, H. Turkdemir, Electrochemical oxidation of textile dye indigo, J. Chem. Technol. Biotechnol. 80 (2005) 916–923.
[9] S. Papic, N. Koprivanac, A.L. Bozic, D. Vujevic, S.K. Dragievic, H. Kusic, I. Peternel, Advanced oxidation processes in azo dye wastewater treatment, Water Environ. Res. 78 (2006) 572–579.
[10] K. Kadirvelu, C. Karthika, N. Vennilamani, S. Pattabhi, Activated carbon from industrial solid waste as an adsorbent for the removal of Rhodamine-B from aqueous solution: kinetic and equilibrium studies, Chemosphere 60 (2005) 1009–1017.
[11] H.M.H. Gad, A.A. El-Sayed, Activated carbon from agricultural by-products for the removal of Rhodamine-B from aqueous solution, J. Hazard. Mater. 168 (2009) 1070–1081.
[12] K. Pazdzior, A. Klepacz-Smolka, S. Ledakowicz, J. Sojka-Ledakowicz, Z. Mrozinska, R. Zylla, Integration of nanofiltration and biological degradation of textile wastewater containing azo dye, Chemosphere 75 (2009) 250–255.
[13] J.A. Zazo, J.A. Casas, A.F. Mohedano, M.A. Gilarranz, J.J. Rodriguez, Chemical pathway and kinetics of phenol oxidation by Fenton's reagent, Environ. Sci. Technol. 39 (2005) 9295–9302.
[14] G.P. Anipsitakis, D.D. Dionysiou, Degradation of organic contaminants in water with sulfate radicals generated by the conjunction of peroxymonosulfate with cobalt, Environ. Sci. Technol. 37 (2003) 4790–4797.
[15] K.H. Chan, W. Chu, Degradation of atrazine by cobalt-mediated activation of peroxymonosulfate: different cobalt counteranions in homogenous process and cobalt oxide catalysts in photolytic heterogeneous process, Water Res. 43 (2009) 2513–2521.
[16] G.P. Anipsitakis, D.D. Dionysiou, Radical generation by the interaction of transition metals with common oxidants, Environ. Sci. Technol. 38 (2004) 3705–3712.
[17] E.R. Bandala, M.A. Pelaez, D.D. Dionysiou, S. Gelover, J. Garcia, D. Macias, Degradation of 2 4-dichlorophenoxyacetic acid (2,4-D) using cobalt-peroxymonosulfate in Fenton-like process, J. Photochem. Photobiol. A-Chem. 186 (2007) 357–363.
[18] A. Rastogi, S.R. Ai-Abed, D.D. Dionysiou, Sulfate radical-based ferrous-peroxymonosulfate oxidative system for PCBs degradation in aqueous and sediment systems, Appl. Catal. B-Environ. 85 (2009) 171–179.
[19] J.K. Richard, M.S. Albert, The oxidation of organic substances by potassium peroxymonosulfate, J. Org. Chem. 25 (1960) 1901–1906.
[20] M. Asilturk, F. Sayilkan, S. Erdemoglu, M. Akarsu, H. Sayilkan, M. Erdemoglu, E. Arpac, Characterization of the hydrothermally synthesized nano-TiO2 crystal-lite and the photocatalytic degradation of Rhodamine B, J. Hazard. Mater. 129 (2006) 164–170.
[21] R. Jain, M. Mathur, S. Sikarwar, A. Mittal, Removal of the hazardous dye rhodamine B through photocatalytic and adsorption treatments, J. Environ. Manage. 85 (2007) 956–964.
[22] J.C. Mirsalis, C.K. Tyson, K.L. Steinmetz, E.K. Loh, C.M. Hamilton, J.P. Bakke, J.W. Spalding, Measurement of unscheduled DNA synthesis and S-phase synthesis in rodent hepatocytes following in vivo treatment: Testing of 24 compounds, Environ. Mol. Mutagenesis 14 (1989) 155–164.
[23] P. Neta, V. Madhavan, H. Zemel, W.F. Richard, Rate constants and mechanism of reaction of sulfate radical anion with aromatic compounds, J. Am. Chem. Soc. 99 (1977) 163–164.
[24] W.P. Ting, M.C. Lu, Y.H. Huang, Kinetics of 2,6-dimethylaniline degradation by electro-Fenton process, J. Hazard. Mater. 161 (2009) 1484–1490.
[25] N. Masomboon, C. Ratanatamskul, M.C. Lu, Chemical oxidation of 2,6-dimethylaniline in the Fenton Process, Environ. Sci. Technol. 43 (2009) 8629–8634.
[26] L.B. Donald, O.E. John, The kinetics and mechanism of the decomposition of Caro's acid, J. Am. Chem. Soc. 78 (1956) 1125–1129.
[27] I.M. Kolthoff, I.K. Miller, The kinetics and mechanism of the decomposition of the persulfate ion in aqueous medium, J. Am. Chem. Soc. 73 (1951) 3055–3059.
[28] K.C. Huang, A.C. Richard, E.H. George, Kinetics of heat-assisted persufate oxidation of methy tert-butyl ether(MTBE), Chemosphere 49 (2002) 413–420.
[29] T.K. Lau, W. Chu, N.J.D. Graham, The aqueous degradation of butylated hydroxyanisole by UV/S2O8^2-: Study of reaction mechanisms via dimerization and mineralization, Environ. Sci. Technol. 41 (2007) 613–619.
[30] G.P. Anipsitakis, D.D. Dionysiou, M.A. Gonzalez, Cobalt-mediated activation of peroxymonosulfate and sulfate radical attack on phenolic compounds. Implications of chloride ions, Environ. Sci. Technol. 40 (2006) 1000–1007.
[31] C.A. Delcomyn, K.E. Bushway, M.V. Henley, Inactivation of biological agents using neutral oxone-chloride solutions, Environ. Sci. Technol. 40 (2006) 2759–2764.
[32] J.N. Stuart, A.L. Goerges, J.M. Zaleski, Characterization of the Ni(III) intermediate in the reaction of (1,4,8,11-tetraazacyclotetradecane)nickel(II) perchlorate with KHSO5: implications to the mechanism of oxidative DNA modification, Inorg. Chem. 39 (2000) 5976–5984.
[33] N. Narender, P. Srinivasu, S.J. Kularni, K.V. Raghavan, Highly efficient, para-selective oxychlorination of aromatic compounds using potassium chloride and Oxone (R), Synth. Commun. 32 (2002).